

# Nanosprings harvest light more efficiently

TURAL KHUDIYEV<sup>1</sup> AND MEHMET BAYINDIR<sup>1,2,3,\*</sup>

<sup>1</sup>UNAM-National Nanotechnology Research Center, Bilkent University, 06800 Ankara, Turkey

<sup>2</sup>Institute of Materials Science and Nanotechnology, Bilkent University, 06800 Ankara, Turkey

<sup>3</sup>Department of Physics, Bilkent University, 06800 Ankara, Turkey

\*Corresponding author: bayindir@nano.org.tr

Received 25 May 2015; revised 10 August 2015; accepted 10 August 2015; posted 11 August 2015 (Doc. ID 241559); published 10 September 2015

Nanotechnology presents versatile architectural designs for the purpose of utilization as a building block of 1D optoelectronic nanodevices because current nanowire-based schemes require more effective solutions for low absorption capacity of nanoscale volumes. We report on the potential of nanospring absorbers as an alternative light-harvesting platform with significant advantages over conventional nanowires. Absorption capacity of nanospring geometry is found to be superior to cylindrical nanowire shape. Unlike nanowires, they are able to trap a larger amount of light thanks to characteristic periodic behavior that boosts light collection for the points matched with Mie resonances. Moreover, nanospring shape supplies compactness to a resulting device with area preservation as high as twofold. By considering that a nanospring array with optimal periods yields higher absorption than individual arrangements and core-shell designs, which further promote light collection due to unique antireflection features of shell layer, these nanostructures will pave the way for the development of highly efficient self-powered nanosystems. © 2015 Optical Society of America

**OCIS codes:** (290.4020) Mie theory; (310.6628) Subwavelength structures, nanostructures; (040.5350) Photovoltaic; (350.2450) Filters, absorption.

<http://dx.doi.org/10.1364/AO.54.008018>

## 1. INTRODUCTION

Nanotechnology enables the production of efficient photosensors utilizing emerging features of nanoscale materials. One-dimensional nanostructures, especially cylindrical nanowires are thoroughly engineered for novel optoelectronic devices, and efforts on many of these shapes have grown remarkably [1,2]. Photosensors of nanometer scale benefits from optical (Mie) resonances, high conversion efficiency, and significant material conservation when compared with bulk devices. However, many of these nanoscale devices [3–8] (e.g., photovoltaics, photodetectors) have the problem of insufficient absorption amount due to the limit on the material absorption capacity and the small volume of individual nanowires. Therefore, 1D photosensors require more efficient absorber platforms in order to effectuate working of the advanced nanodevices. Moreover, compactness of the utilized power-supplying nanostructures is another crucial aspect of the design in the self-powered nanosystems [9,10]. Therefore, engineering of the nanodevices should consider the balance between the absorption capacity and the space saving within the system.

Several strategies—including engineering light absorption in the nanowire [11,12], morphological design [13,14], and multi-absorber patterns [15–17]—are well known for enhancing absorption capability of individual nanowires. Alternative ap-

proaches to enhance the absorption efficiency, such as light trapping techniques using low-index or metallic nanostructures, also have been widely investigated for their accumulation performance [18,19]. It is worth noting, however, that constructing large-scale and efficient optoelectronic devices should rely on selection of their appropriate nano-building blocks. For instance, many examples in natural systems show that complex nanoarchitectures provide more functions and higher efficiency than simple systems that are constructed from basic or regular structures. Similarly, nanostructure-based photosensor design should consider more suitable and efficient architectures. However, such complexities (e.g., chiral or asymmetric structures) are also required to be reflected in practical devices. Even though nanotechnology satisfies the production requirements and characterization of some of such complex platforms [20–23], it could not provide powerful solutions to the issues, including large-area scalability, alignment, addressability, etc. Therefore, besides the proof-of-concept demonstration of novel devices, these proposed designs should also meet the requirements of their applicability (efficiency, cost-effectiveness).

Here, we introduce nanospring absorbers as an efficient photosensor platform. Nanosprings are observed to yield significantly higher solar absorption efficiency in comparison with cylindrical nanowires. This is attributed to the unique shape of

the springs, which is able to accumulate a larger amount of light in the vicinity of chiral hot spots. By optimizing structural parameters (e.g., pitch size and diameter) of the nanosprings, we obtain  $\sim 23\%$  absorption enhancement for unpolarized incident light, which is especially important for solar cell design. Besides exhibiting superior absorption capability, these asymmetric schemes are also promising for highly compact nanodevice designs because of their substantial area preservation. The longitudinal size can be shortened to a half while yielding the same power level as obtained in cylindrical nanowires. Nanosprings are also found to be highly advantageous and efficient as a core-shell form (details will be explained later) and can play an important role in the design of large-area systems where array of nanosprings can be even more efficient absorbers than single nanospring absorbers if correct spacings are chosen on a large-area scheme.

## 2. RESULTS

Figure 1(a) represents our nanospring-based photosensor scheme. Interaction of light with nanowire geometry induces emergence of useful optical features unique to nanoscale materials; therefore, these nanostructures have been utilized successfully as a building block of 1D solar cells. They simply take advantage of size-dependent Mie resonances through the nanowire periphery. This makes nanowire a more efficient absorber than their planar counterparts. However, nanotechnology provides versatile design options that may have even more effective absorption capability than cylindrical geometry. Nanosprings are emerging as an optical nanoelement and can be used in different photonics applications [24–29]. A nanospring scheme is demonstrated to have significant potential in 1D nanostructure-based optoelectronics and many advantageous features compared with nanowire geometry. Absorber material in nanospring and reference nanowire schemes composed of well-known amorphous silicon glass (a-Si) and their radial size selected as  $d = 200$  nm for the utilization throughout the theoretical investigations. Light incident on the absorber couples to the nanostructure radial axis via the leaky-mode behavior where the trapped light resonantly oscillates through multiple total internal reflections on the periphery and induces resonant absorption process. Nanosprings are chiral nanostructures that can be formed by twisting wire shaped around the longitudinal axis. Similar to the nanowire geometry, they are also able to support Mie resonances in a characteristic behavior. This makes many regular nanostructures as well as our chiral platform to effectively absorb light, especially at points corresponding to the Mie resonances. However, nanospring geometry uniquely enhances absorption capability of a structure due to the presence of additional effects. This enhancement factor can be as high as  $\sim 23\%$  for unpolarized light. Corresponding near-field profiles of optical resonances exhibit this increment as amplified localized intensity throughout the nanospring geometry. This rise is reflected as an absorption enhancement for TE and TM polarizations [Figs. 1(b)–1(d)]. The longitudinal field profiles representing  $TE_{11}$  and  $TM_{21}$  modes at wavelengths of 560 and 700 nm further clarify the absorption process in a nanospring geometry [Fig. 1(e)]. The light

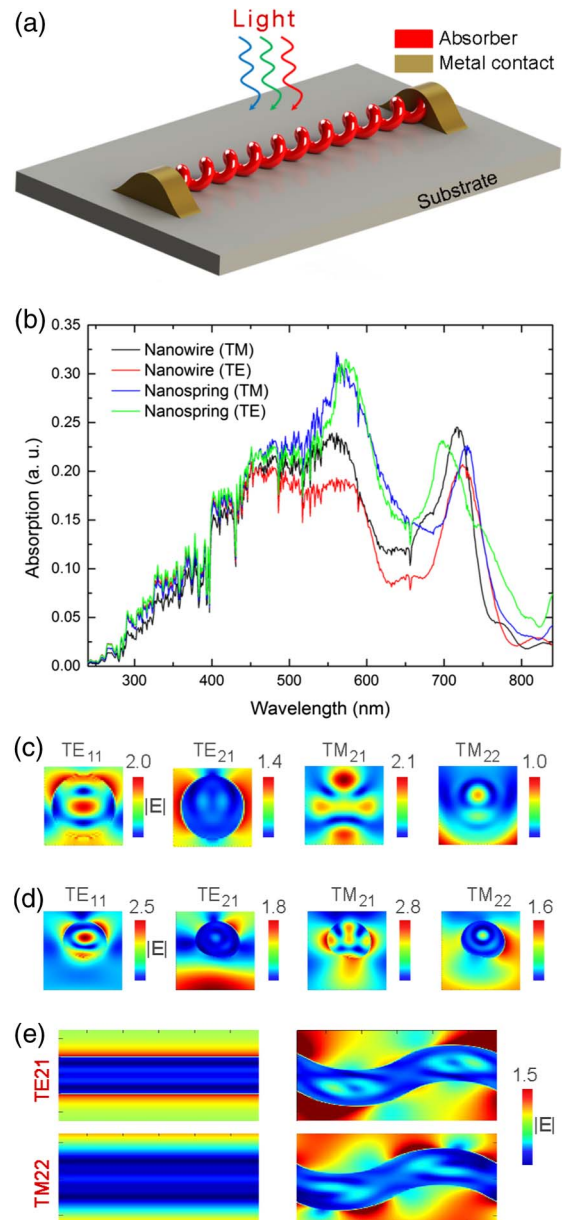


**Fig. 1.** Nanosprings can absorb light more efficiently. (a) Scheme represents prototype of utilized device that is composed of bare nanospring photodetectors placed on a glass substrate and metal contacts in order to collect charges. Light incidents from top of the nanostructure. (b) Photocurrent generated in this scheme and in nanowire geometry for the TE and TM polarization mode. Photocurrent in nanospring case is boosted by  $\sim 23\%$  (for TM 17% and TE 29%). The peaks are due to the optical Mie resonances. (c) and (d) Resonance field profile of the modes at peaks of 560 and 700 nm in the nanowire case and nanospring case in (b). It can be seen that the nanosprings also support these types of resonance; particularly, the  $TE_{11}$  and  $TM_{21}$  modes are clearly visible from near-field profiles of corresponding resonances. (e) Comparison of the longitudinal field profiles between the nanowire (left) and nanospring (right) exhibits that the nanosprings are able to support a larger amount of light, which adds further enhancement on absorption capacity of bare nanowire.

uniquely couples to the nanospring geometry, alters the Mie resonances, and induces chiral hot spots in a way that the overall light accumulation is boosted.

Origin of the additional enhancement can be easily explained and revealed when the absorption map is plotted in the broad range of nanospring pitch sizes. Particularly for selected nanowire and a nanospring with diameter of 200 nm, the induced resonant absorption peaks appear at the peak wavelengths of  $\sim 500$  nm (TE<sub>21</sub>, TM<sub>22</sub>) and  $\sim 700$  nm (TE<sub>11</sub>, TM<sub>21</sub>). Absorption maps are derived for the TE and TM polarizations in 300–1000 nm nanospring period range and reveal the fact that additional enhancement appears when a nanospring period matches one of the existing leaky-mode Mie resonances. Dashed lines marked with “1” and “2” clearly show this resonant matching effect [Fig. 2(a)]. It can be observed that, when the nanospring periods of  $P = 500$  nm (“1”) and 700 nm (“2”) overlap the resonant absorption points of the Mie phenomenon ( $\lambda = 500$  and 700 nm), the light absorption is increased accordingly. These arrangements are potentially applicable to other orders of Mie resonances and wire radii that require matching of a nanospring period with those of resonant points for design of efficient nanospring photosensors.

However, in practical cases this is not the point in question because resonant absorption points are adequately broad and tolerable for broad nanospring periodicity. By calculating total absorption over a wavelength range of 240–840 nm, we can observe that nanospring absorption is superior to nanowires for both types of polarization and in a broad range of the nanospring period [Fig. 2(b)]. It is worth noting that maximal absorption requires not only matching of the period with single resonant points, but proper interplay between existing resonances and nanospring periods may provide even higher total absorption capacity. We observe that maximum total absorption occurs for the period of  $\sim 560$  nm (point that corresponds to intermediate region of resonant wavelengths).

To further optimize the nanospring absorption performance, we also investigate the effect of nanospring diameter ( $D$ ). This design parameter is distinct from the wire diameter itself, which is set as  $d = 200$  nm throughout the calculations. A map of nanospring absorption is plotted in the diameter range of 20–1000 nm for both types of polarization [Fig. 3(a)]. Maximum absorption is observed to be in the diameter ( $D$ ) range of 50–200 nm. During these calculations, pre-obtained optimal periodicity value ( $P = 560$  nm) is used. It is worthwhile to note that, when nanospring diameter approaches zero, geometry converges to a conventional nanowire shape; therefore, at these smaller diameters, total absorption is closest to the black (TE) and red (TM) lines representing absorption of nanowire geometry [Fig. 3(b)]. Furthermore, for larger diameter values, the absorption performance starts to drop. Nanospring geometry is even inferior to cylindrical nanowire in its absorption amount when  $D$  is above 400 nm. By considering  $P = 560$  nm and  $D = 140$ , we observe one of the maximal absorption enhancements of nanosprings compared with nanowires, where for TE and TM polarizations this amplification is around  $\sim 25.5\%$  and  $\sim 19\%$ , respectively.

A nanospring absorber also can be designed for large-area applications. Individual elements of a large-area scheme are selected from optimal size parameters ( $P = 560$  nm,  $D = 70$  nm). Pitch-dependent absorption characteristics of these nanostructures are demonstrated in Fig. 4(a). Light absorption

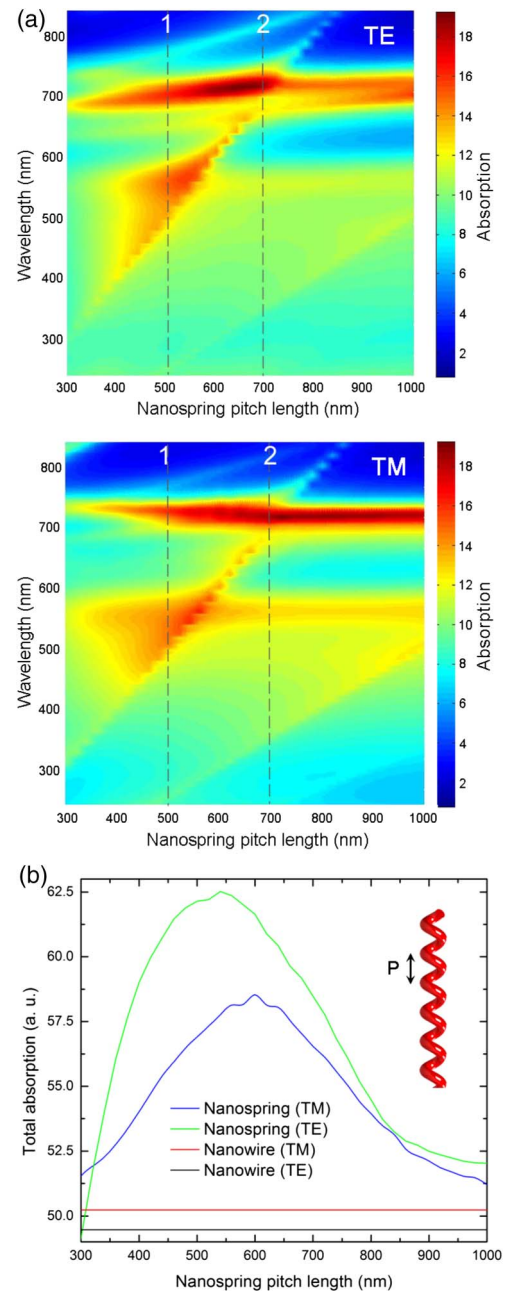


**Fig. 2.** Effect of nanospring pitch length. (a) Nanospring pitch length ( $P$ ) is one of the main factors that alter the absorption profile and capacity of absorber medium. Map of absorption that takes the pitch length factor into consideration assists to observe most efficient portions (i.e., suitable pitch sizes) for the utilization in the design. It is worthwhile to note that, when nanospring pitch size matches with one of the supported Mie resonances, absorption of nanostructure significantly increases. However, overall maximal absorption should be engineered according to proper interplay of existing resonances. (b) Highest absorption amount found to be around at  $P = 560$  nm for unpolarized light case. At these points, absorption is superior to conventional nanowire shape of same length and diameter.

becomes maximal when the spacing values overlap with nanowire resonances similar to the nanospring pitch length matching process in Fig. 2. In array form, for both types of

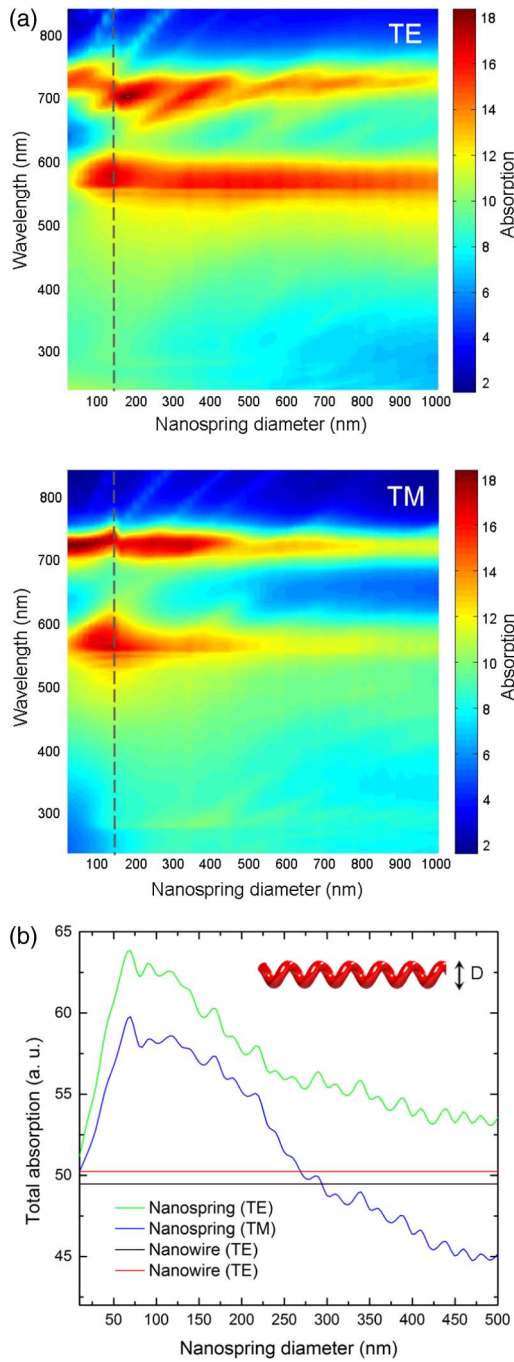


**Fig. 3.** Effect of nanospring diameter. (a) Nanospring diameter ( $D$ ) is another parameter that affects maximal absorption point. By altering  $D$  in the 20–1000 nm range, we determine absorption that yields highest absorption amount. (b) This range corresponds with nanospring diameter of 100–200 nm. Nanosprings at these optimized sizes utilizes localized near-field spots unique to the spring shape. Using optimized nanospring pitch values and diameters, absorption enhancement capacity can be further increased to the amount of  $\sim 25.5\%$  and  $\sim 19\%$  for TE and TM polarizations, respectively.

polarizations, nanosprings absorb light effectively with over 20% more than their single form. Another critical advantage of the nanosprings is their compactness. Along the longitudinal axis, they can save more than 25% area in our case, and the

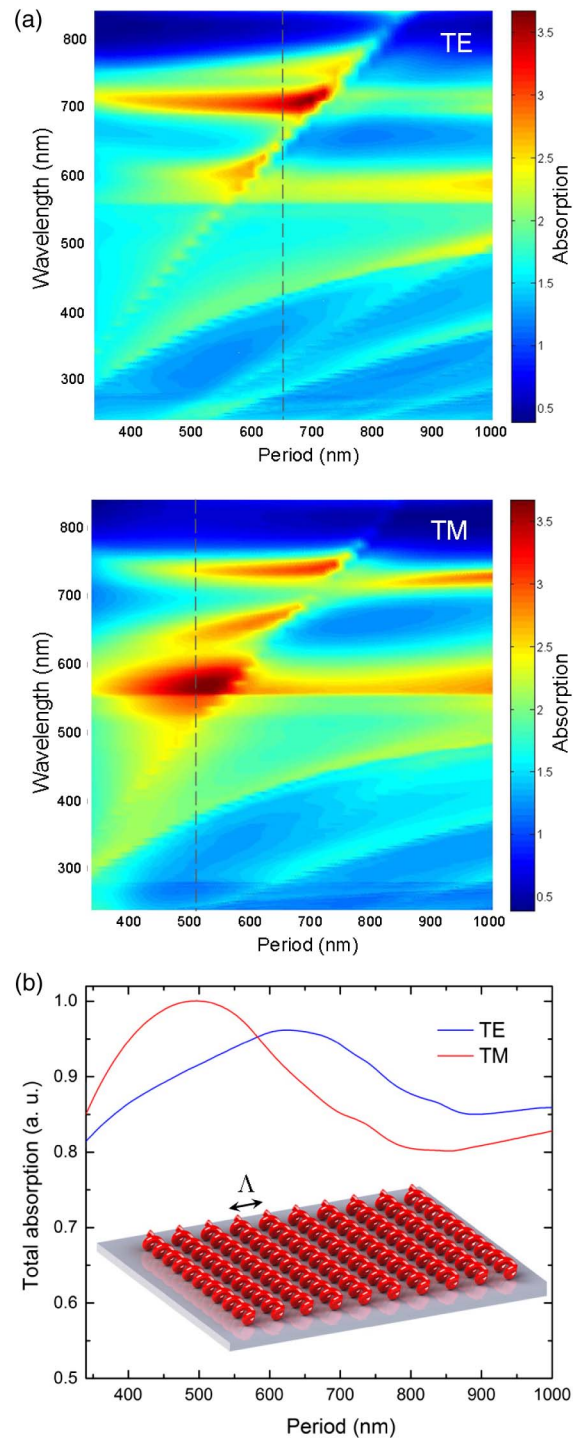


**Fig. 4.** Array of nanosprings. (a) Nanosprings can play a role in large-area configurations if correct periods ( $\Lambda$ ) are selected. These spacings can make an array to absorb light even more efficiently than individual ones. (b) Calculations demonstrate that, by selecting period value of 600 nm, it is possible to construct a highly efficient photo-sensor scheme. Absorption amount in array case enhanced by the factor of 13.5% for TE polarization and 25% for TM polarization in comparison with configuration that is constructed by unaffected array of individual nanosprings.

value is even higher if optimal design parameters are used. For example, by selecting nanospring radius as 150 nm, we can save 50% area and still obtain  $\sim 21\%$  absorption enhancement compared with nanowires. Even though this may occur with the expense of increasing radial space, for large-area designs, the interstructural spacings are already required to be larger than these radial dimensions. Optimal period value yielding maximal absorption for large-area applications can be selected as  $\sim 600$  nm, even though maxima of individual polarizations are at 500 nm (TM) and 650 nm (TE) [Fig. 4(b)].

A nanospring-based photosensor design can be even more effective when we add a low-index (e.g.,  $\text{SiO}_2$ , polymers) shell to it. A core-shell scheme is frequently considered in current nanowire-based photovoltaic designs for the purpose of obtaining more efficient absorption because the shell layer is able to reduce reflected light significantly thanks to the characteristic light accumulation and the slight adiabaticity in refractive indices throughout the propagation over core-shell components. Design of the nanospring-based photosensor platform in an individual or array form can utilize the benefit of shell-induced light trapping as well. We utilize 500 nm diameter of the  $\text{SiO}_2$  shell and embed an optimized nanospring design inside it [Fig. 5(a)]. A core-shell nanospring scheme

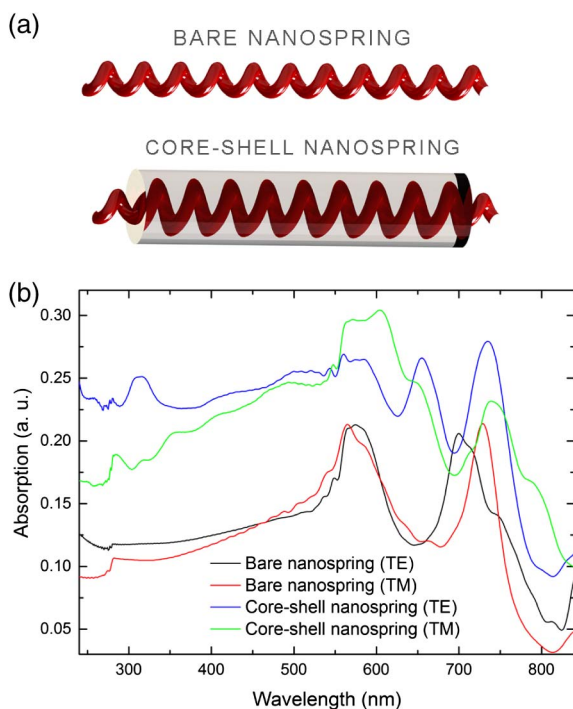


**Fig. 5.** Core-shell nanosprings. (a) Because many of current nanowire-based photosensors take advantage of core-shell scheme, nanosprings also can be designed as a core-shell configuration for observing even more efficient performance. (b) We find that for TE and TM polarizations, absorption significantly enhanced via the light trapping features of low-index shell region. This enhancement is  $\sim 70\%$  (for TE and TM polarization enhancements are 68% and 72%, respectively) for current design (for shell thickness of 500 nm and material composition of  $\text{SiO}_2$ ) and can be optimized to reach even higher values by choosing more optimal material parameters (e.g., shell material with more suitable optical constants and thicknesses).

can supply additional 70% absorption enhancement over a bare nanospring platform [Fig. 5(b)]. This value can be easily exceeded if shell thickness and the material's optical constants are optimized. By considering the optimal period that is required to be  $\sim 600$  nm and optimal shell thickness, we can conclude that our photosensor designs can significantly satisfy practicality and cost-effectiveness required in novel optoelectronic device fabrication.

### 3. CONCLUSION AND DISCUSSION

To conclude, we propose the nanospring-based absorbers for the utilization as a novel photosensor platform and discuss the optimization of the design in different circumstances. Nanospring absorbers are designed effectively by optimizing their structural parameters (e.g., nanospring period and radius), which are unique to these chiral shapes. We find that nanosprings can provide 23% total absorption enhancement in comparison with conventional nanowire absorbers and can save an area as high as 50%. Nanospring absorbers can effectively take advantage of two distinct effects: resonant Mie absorption and resonance matching. Nanosprings are promising to serve as a high-power photosensor scheme (e.g., photovoltaics, photodetectors), which can be exploited in the nanoscale systems to effectuate working of self-powered nanodevices, and power efficiencies, which can be further amplified by considering the potential of core-shell structures with 70% absorption enhancement or array design (i.e., by implementing optimal pitch sizes) with 20% additional absorption capacity than individual absorbers.

Why nanosprings in practical cases would be preferred to the well-known nanowire geometry though fabrication of nanospring geometry seems to be challenging in comparison with conventional nanowire shapes (many of the existing nanofabrication techniques have been optimized for producing regular geometries such as nanowire and nanosphere)? The answer is that production of nanosprings can be extended from nanowire fabrication through a simple transition process at no additional cost, and the yield is as efficient as that of cylindrical nanowires. One such technique has been recently developed and relies purely on heat-treatment processes [30,31]. Iterative size reduction (ISR) technique, which is based on multiple and serial size-reduction process of a macroscale structure, is able to satisfy basic requirements existing in nanowire fabrication. By using this technique, one can even fabricate indefinitely long, uniform, globally ordered nanostructures that are controlled from macroscale sizes in their arrangements (i.e., circular array of nanostructures, monolayer nanostructures, core-shell scheme [32], and photonic-crystal-type [33] nanowire arrangements, which can be easily designed at macroscale sizes). Originality of nanospring fabrication appears in a subsequent fabrication step where nanowires produced by ISR technique are subjected to heat treatment. By setting temperature above the glass transition point of utilized materials, it is possible to fabricate many useful and difficult-to-produce nanostructures, including nanospring schemes with their optimal size parameters for the utilization in photosensor applications. The technique in question takes advantage of an instability phenomenon that may occur in solid materials during their

softening. While core material is reaching proper viscosity level, surface tension between cladding and core region induces formation of spiral shapes. Nanospring dimensions (i.e., pitch size and diameter) can be controlled easily by setting proper heating duration and temperature. Another critical point is regarding the chirality of an absorber such that either right-handed or left-handed nanosprings can be used for our design because they do not affect absorption profiles and yield exactly the same result (hence, this will not be one of the concerns in device design). Therefore, by considering higher absorption efficiency (i.e., for bare and core-shell designs), flexible design parameters (i.e., tolerable periodicity and nanospring diameter, independency from chirality, etc.), and compactness of proposed nanospring geometry, we believe these promising shapes will pave the way toward the development of highly efficient self-powered compact nanosystems and can even be complementary in large-area high-power photovoltaics systems.

**Funding.** European Research Council (ERC) (307357).

## REFERENCES

1. T. J. Kempa, R. W. Day, S. K. Kim, H. G. Park, and C. M. Lieber, "Semiconductor nanowires: a platform for exploring limits and concepts for nano-enabled solar cells," *Energy Environ. Sci.* **6**, 719–733 (2013).
2. E. C. Garnett, M. L. Brongersma, Y. Cui, and M. D. McGehee, "Nanowire solar cells," *Annu. Rev. Mater. Res.* **41**, 269–295 (2011).
3. H. Kind, H. Yan, B. Messer, M. Law, and P. Yang, "Nanowire ultraviolet photodetectors and optical switches," *Adv. Mater.* **14**, 158–160 (2002).
4. Z. Fan, J. C. Ho, Z. A. Jacobson, H. Razavi, and A. Javey, "Large-scale, heterogeneous integration of nanowire arrays for image sensor circuitry," *Proc. Natl. Acad. Sci. USA* **105**, 11066–11070 (2008).
5. W. S. Wong, S. Raychaudhuri, R. Lujan, S. Sambandan, and R. A. Street, "Hybrid Si nanowire/amorphous silicon FETs for large-area image sensor arrays," *Nano Lett.* **11**, 2214–2218 (2011).
6. K. Ul Hasan, N. H. Alvi, J. Lu, O. Nur, and M. Willander, "The origin of the red emission in n-ZnO nanotubes/p-GaN white light emitting diodes," *Nano. Res. Lett.* **6**, 130 (2011).
7. H. Wang, "High gain single GaAs nanowire photodetector," *Appl. Phys. Lett.* **103**, 093101 (2013).
8. G. Chen, Z. Liu, B. Liang, G. Yu, Z. Xie, H. Huang, B. Liu, X. Wang, D. Chen, M.-Q. Zhu, and G. Shen, "Single-crystalline p-type Zn<sub>3</sub>As<sub>2</sub> nanowires for field-effect transistors and visible-light photodetectors on rigid and flexible substrates," *Adv. Funct. Mater.* **23**, 2681–2690 (2013).
9. S. Xu, Y. Qin, C. Xu, Y. Wei, R. Yang, and Z. L. Wang, "Self-powered nanowire devices," *Nat. Nanotechnol.* **5**, 366–373 (2010).
10. B. Tian, X. Zheng, T. J. Kempa, Y. Fang, N. Yu, G. Yu, J. Huang, and C. M. Lieber, "Coaxial silicon nanowires as solar cells and nanoelectronic power sources," *Nature* **449**, 885–889 (2007).
11. L. Cao, J. S. White, J. S. Park, J. A. Schuller, B. M. Clemens, and M. L. Brongersma, "Engineering light absorption in semiconductor nanowire devices," *Nat. Mater.* **8**, 643–647 (2009).
12. M. L. Brongersma, Y. Cui, and S. Fan, "Light management for photovoltaics using high-index nanostructures," *Nat. Mater.* **13**, 451–460 (2014).
13. S. K. Kim, K. D. Song, T. J. Kempa, R. W. Day, C. M. Lieber, and H. G. Park, "Design of nanowire optical cavities as efficient photon absorbers," *ACS Nano* **8**, 3707–3714 (2014).
14. S. K. Kim, R. W. Day, J. F. Cahoon, T. J. Kempa, K. D. Song, H. G. Park, and C. M. Lieber, "Tuning light absorption in core/shell silicon nanowire photovoltaic devices through morphological design," *Nano Lett.* **12**, 4971–4976 (2012).
15. W. F. Liu, J. I. Oh, and W. Z. Shen, "Light absorption mechanism in single c-Si (core)/a-Si (shell) coaxial nanowires," *Nanotechnology* **22**, 125705 (2011).
16. W. Q. Xie, W. F. Liu, J. I. Oh, and W. Z. Shen, "Optical absorption in c-Si/a-Si: H core/shell nanowire arrays for photovoltaic applications," *Appl. Phys. Lett.* **99**, 033107 (2011).
17. H. Kallel, A. Chehaidar, A. Arbouet, and V. Paillard, "Enhanced absorption of solar light in Ge/Si core-sheath nanowires compared to Si/Ge core-sheath and Si<sub>1-x</sub>Ge<sub>x</sub> nanowires: a theoretical study," *J. Appl. Phys.* **114**, 224312 (2013).
18. W. F. Liu, J. I. Oh, and W. Z. Shen, "Light trapping in single coaxial nanowires for photovoltaic applications," *IEEE Electron Device Lett.* **32**, 45–47 (2011).
19. X. Hua, Y. Zeng, and W. Z. Shen, "Semiconductor/dielectric half-coaxial nanowire arrays for large-area nanostructured photovoltaics," *J. Appl. Phys.* **115**, 124309 (2014).
20. S. V. N. T. Kuchibhatla, A. S. Karakoti, D. Bera, and S. Seal, "One dimensional nanostructured materials," *Prog. Mater. Sci.* **52**, 699–913 (2007).
21. D. J. Bell, L. Dong, B. J. Nelson, M. Golling, L. Zhang, and D. Grützmacher, "Fabrication and characterization of three-dimensional InGaAs/GaAs nanosprings," *Nano Lett.* **6**, 725–729 (2006).
22. D. Zhang, A. Alkhateeb, H. Han, H. Mahmood, D. N. McIlroy, and M. G. Norton, "Silicon carbide nanosprings," *Nano Lett.* **3**, 983–987 (2003).
23. P. X. Gao and Z. L. Wang, "High-yield synthesis of single-crystal nanosprings of ZnO," *Small* **1**, 945–949 (2005).
24. M. Schäferling, X. Yin, N. Engheta, and H. Giessen, "Helical plasmonic nanostructures as prototypical chiral near-field sources," *ACS Photonics* **1**, 530–537 (2014).
25. V. V. R. Sai, D. Gangadean, I. Niraula, J. M. F. Jabal, G. Corti, D. N. McIlroy, D. E. Aston, J. R. Brannen, and P. J. Hrdlicka, "Silica nanosprings coated with noble metal nanoparticles: Highly active SERS substrates," *J. Phys. Chem. C* **115**, 453–459 (2011).
26. S. Y. Bae, J. Lee, H. Jung, J. Park, and J. P. Ahn, "Helical structure of single-crystalline ZnGa<sub>2</sub>O<sub>4</sub> nanowires," *J. Am. Chem. Soc.* **127**, 10802–10803 (2005).
27. X. L. Wu, Q. Liu, Y. G. Guo, and W. G. Song, "Superior storage performance of carbon nanosprings as anode materials for lithium-ion batteries," *Electrochem. Commun.* **11**, 1468–1471 (2009).
28. D. Grützmacher, L. Zhang, L. Dong, D. Bell, B. Nelson, A. Prinz, and E. Ruh, "Ultra flexible SiGe/Si/Cr nanosprings," *Microelectron. J.* **39**, 478–481 (2008).
29. Z. Y. Zhang, X. L. Wu, L. L. Xu, J. C. Shen, G. G. Siu, and P. K. Chu, "Synthesis, growth mechanism, and light-emission properties of twisted SiO<sub>2</sub> nanobelts and nanosprings," *J. Chem. Phys.* **129**, 164702 (2008).
30. T. Khudiyev, O. Tobail, and M. Bayindir, "Tailoring self-organized nanostructured morphologies in kilometer-long polymer fiber," *Sci. Rep.* **4**, 4864 (2014).
31. M. Yaman, T. Khudiyev, E. Ozgur, M. Kanik, O. Aktas, E. O. Ozgur, H. Deniz, E. Korkut, and M. Bayindir, "Arrays of indefinitely-long, uniform nanowires and nanotubes," *Nat. Mater.* **10**, 494–501 (2011).
32. T. Khudiyev, E. Ozgur, M. Yaman, and M. Bayindir, "Structural coloring in large scale core-shell nanowires," *Nano Lett.* **11**, 4661–4665 (2011).
33. T. Khudiyev, T. Dogan, and M. Bayindir, "Biomimicry of multifunctional nanostructures in the neck feathers of mallard (*Anas platyrhynchos* L.) drakes," *Sci. Rep.* **4**, 4718 (2014).